**MATERIALE PLASTICE**
*https://revmaterialeplastice.ro*
*https://doi.org/10.37358/Mat.Plast.1964*

# Efficient Thermo-Stability and Smoke-Suppression Properties of La Doping Mg-Al LDHs on PVC Nanocomposites

**JINJIE ZHANG[1], BIN XU[1], HENGXU WANG[1], FUPENG JIN[1], JINFENG DAI[1,2*], SHENYUAN FU[1,2 *]**

[1] Department of Materials, College of Engineering, Zhejiang A & F University, 666 Wusu Street, Linan District, Hangzhou 311300, China

[2] National Engineering and Technology Research Center of Wood-based Resources Comprehensive Utilization, 666 Wusu Street, Lin`an District, Hangzhou 311300, China

***Abstract.*** *Despite the advantages of the non-flammable, good performance and low price, poly (vinyl chloride) (PVC) still suffer from poor thermal stability, restricting its melting process and applications. Although addition of some heat stabilizers can be used to improve the low thermal stability, so far, they normally compromise the environmental issues and smoke density of PVC during combustion. In this work, a series of La doping Mg-Al layered double hydroxides (LaLDHs) with different molar ratio of $La^{3+}$ / $Al^{3+}$ were successfully synthesized by coprecipitation-hydrothermal method and characterized by X-ray diffraction (XRD), Fourier transform infrared spectrum (FT-IR), Scanning Electron Microscopy (SEM) and Transmission electron microscopy (TEM). The results showed that the as-prepared LaLDHs exhibit plate-like morphology with a lateral size around 100-180 nm. The different as-prepared LaLDHs were introduced into PVC as heat stabilizer to prepare PVC nanocomposites. The thermal stability and smoke suppression of PVC nanocomposites were investigated by TGA, thermal aging, Congo red and smoke density rating test (SDR), respectively. All the results demonstrated that PVC-LaLDHs2 nanocomposites containing 2% LaLDHs2 (the molar ratio of $La^{3+}$ / $Al^{3+}$ is 1 / 3) were optimized, which achieved the maximal $T_{50\%}$ value of 337.2 °C, minimal SDR value of 45.6%, and prolonged the thermal aging time from less than 10mins to 90mins, respectively thermal stability time from 1242s to 2751s. In addition, the tensile strength and elastic modulus of PVC-LaLDHs2 respectively increased by 84.4% (56.6 MPa) and 75.5% (1019.4 MPa) with little affecting elongation at break of PVC.*

***Keywords:*** *LDHs (layered double hydroxides); rare earth ions; thermal stability; smoke suppression; poly (vinyl chloride)*

## 1. Introduction

Poly (vinyl chloride) (PVC) is one of the five biggest general thermoplastics and widely applied in various fields such as construction, chemical, decoration, packaging, and cable industry for its desirable physicochemical properties, easy acceptance and workability [1-4]. Unfortunately, PVC is inherently sensitive to heat with poor thermal stability and tend to colorate with thermal degradation during its processing [5, 6], and that restricts the application in many areas, especially in electrical fields. In addition, PVC, under the influence of heat source and energy radiation, suffers autocatalytic dehydrochlorination reactions and initial reactions of dehydrochlorination, further accelerating the decomposition of the polymer, even resulting in great black smoke and toxic gases during combustion, although PVC is well known self-extinguishing polymer [6].

To overcome these limitations, addition of heat stabilizer during the processing is a key factor to improve the thermal stability of PVC. Conventional heat stabilizer used in PVC is lead salts, which have been challenged and restricted by environmental legislations because of the heavy metals with toxicity on organisms and environment [7]. Metal soaps have excellent transparency and lubricity, while their efficiency of thermal stability is low when they are used alone [8]. As a high-efficiency, non-toxicity, and synergetic effect with other heat stabilizers, Rare-earth stabilizer attracts increasing attention and share fascinating prospect [9, 10].

**email: jinfengdai0601@gmail.com, fshenyuan@sina.com*

However, the initial stabilization effect of rare-earth stabilizer is not satisfying, as well as its expensive price. For these reasons, a new heat stabilizer with non-toxic, eco-friendly and economical that could substantially improve initial stabilization efficiency is urgently needed.

Recent years, Layered double hydroxides (LDHs) with exchangeable bimetallic cations and interlayer anions have been given a great research potential and application prospect for its special structure and various properties [11-15]. As a promising thermal stabilizer, LDHs exhibits a desired effect of enhancement on thermal stability of PVC. Liu et al. [16] have reported that alkalescency and layered structure of Mg-Al LDHs could scavenge the HCl produced in the degradation of PVC [17]. Unfortunately, this chemical composition of Mg-Al LDHs is difficult to suppress the initial discoloration and dechlorination of PVC, because of its inability to react with labile chlorine atoms (such as allyl chloride) [10, 18]. Wang et al. [19] showed that Zn-doped Mg-Al LDHs could efficiently improve the initial and long-term thermal stability of PVC nanocomposites. However, the unsuitable production $ZnCl_2$ could catalyze the degradation of PVC, resulting in malignant decomposition of PVC and making PVC turn black suddenly, namely phenomenon of "zinc burning" [20]. Different from the above works, Yang et al. [21] prepared rare-earth ions doped LDHs, and found that rare-earth ions doped LDHs not only avoid to occur "zinc burning", but also the effect of thermal stability improve significantly, which benefited from the catalytic and synergistic effect of rare-earth ions [22]. Moreover, the content of rare-earth ions has a great influence on the thermal stability of doped LDHs, and modulation of the ratio of metal ions plays a crucial role in the heat stabilizer.

Consistently, LDHs has been considered as one of the most potential flame-retardant and smoke suppression material for polymers owing to its unique chemical composition and layered structure [20, 23, 24]. Therefore, we herein attempt to dope rare-earth element Lanthanum into Mg-Al LDHs for synthesizing novel heat stabilizer with manipulating the molar ratio of metal ions. It can be presumed that introduction of rare-earth element Lanthanum doped Mg-Al LDHs will contribute to an improvement of PVC thermal stability and, at the same time, it can be expected that such a heat stabilizer will reduce the smoke density of PVC during combustion. In addition, introduction of rare-earth element Lanthanum doped Mg-Al LDHs to the PVC nanocomposites will even contribute to the mechanical properties of the proposed PVC nanocomposites. Above all, assessment of these modifications is the main target of this research in the present work.

## 2. Materials and methods

### 2.1. Materials

The pure PVC powders (SG-8) were obtained from Xinjiang Tianye (group) Co., Ltd. Nano calcium carbonate ($CaCO_3$) was industrial grade supplied by Jiangxi huaming nano calcium carbonate co., LTD. $Mg(NO_3)_2{\cdot}6H_2O$, $Al(NO_3)_3{\cdot}9H_2O$, $La(NO_3)_3{\cdot}6H_2O$, NaOH, dioctyl phthalate (DOP), epoxidized soya bean oil (ESO), octadecanoic acid calcium salt ($Ca(st)_2$) and octadecanoic acid zinc salt ($Zn(st)_2$) were purchased from Shanghai Macklin Biochemical Co., Ltd,. All the regents were analytical grade and used as received without any further purification.

### 2.2. Preparation of LaLDHs

The LaLDHs used in this work were synthesized using a coprecipitation-hydrothermal method. Generally, a 50 mL ultrapure water containing 0.03 mol $Mg(NO_3)_2{\cdot}6H_2O$ and 0.01 mol $M^{3+}$ metal salts ($Al(NO_3)_3{\cdot}9H_2O$ and $La(NO_3)_3{\cdot}6H_2O$) were added drop-wise to another 100 mL ultrapure water at a molar $M^{2+}$:$M^{3+}$ratio of 3. In addition, the $La^{3+}/Al^{3+}$ molar ratio was adjusted to 1:2, 1:3, 1:4, 1:5 for comparison. In the meantime, the *p*H of the system was strictly controlled at 10 using 0.1 M NaOH solution at 80$^o$C with vigorous stirring under nitrogen. The resulting mixture was transferred to a Teflon-lined autoclave that was sealed in a stainless steel shell after 4h. The vessel was hydrothermally treated at 150$^o$C for 10h. And then the obtained samples were washed with deionized water until *p*H=7. Later the samples were washed with ethanol 1-2 times. Finally, all the as-prepared samples (namely, LaLDHs1, LaLDHs2, LaLDHs3 and LaLDHs4) were dried at 80 $^o$C overnight.

### 2.3. Preparation of PVC-LaLDHs nanocomposites

PVC-LaLDHs nanocomposites were prepared by melting and blending PVC powder with DOP, ESO, $CaCO_3$, $Ca(st)_2$, $Zn(st)_2$, and a certain amount of as-prepared LaLDHs using a ThermoHaake Torque Rheometer with a rotor speed of 45 rpm at 170°C for 10 min. Subsequently, the specimens were thermo-compressed at 175°C to form the samples of suitable size for tests. The basic formula was designed as follow: PVC 100g, DOP 5g, ESO 5g, $CaCO_3$ 10g, $Ca(st)_2$ and $Zn(st)_2$ 1g, and the as-synthesized LaLDHs 2g.

### 2.4. Characterization

The crystalline structure of samples was characterized by powder X-ray diffraction using a XRD-6000 diffractometer (Shimadzu, Japan) with Cu Kα radiation ($\lambda = 1.542$ Å) at a scanning rate of $2\theta = 2^o$ / min. FT-IR spectra were recorded on a Bruker Vector 22 FT-IR spectrometer in the range of 400 - 4000 $cm^{-1}$ using solid KBr pellet. Scanning Electron Microscopy (SEM, FEI-SEM, Japan) was employed to observe the microstructure of as-obtained LaLDHs as well as their dispersion in the PVC matrix with an accelerating voltage of 15 kV. The morphology of samples was investigated by Transmission Electron Microscopy (TEM, JEM-1200EX, Japan) at 200 kV. The samples were dispersed in ethanol by an ultrasonic treatment and then dropped onto copper TEM grip. The thermal stability of all PVC / LaLDHs nanocomposites was carried out and analyzed via a thermogravimetric analyzer (209F1, NETZSCH, Germany) at a heating rate of 20°C / min (from 30 to 700°C) under flowing $N_2$. The static thermal aging test was performed as follow: the resulting nanocomposites were molded to a film with 1mm thickness, and cut into 2 cm × 2 cm × 1 mm strips. These strips were placed in a thermal aging test box at 195 ± 1 $^oC$ and subjected to static thermal aging, which is according to the ISO 305-1990 standard. The strips were taken out of the box every 10 min and recorded by digital photo. The Congo red test was analyzed according to ISO 182 / 1-1990 (E) standard. The target specimens were put into a tube with Congo red test paper located at 2 cm above the samples. The tube was heated with an oil bath at 180 ± 1$^oC$. The time when Congo red test paper began to turn blue was defined as static stability time for evaluating static thermal stability of the PVC / LaLDHs nanocomposites. The smoke density (SDR) of all nanocomposites was performed on a JCY-2 instrument (Nanjing Jiangning Analysis Instrument CO., LTD., China) according to ASTM D2843-1993 standard. The mechanical properties of the PVC-LaLDHs nanocomposites were measured following ASTM 638-03 in a universal testing machine (MTS SYSTEMS Co., Ltd, China) with a cross-head rate of 5.0 mm/min at room temperature, and all samples were averaged in quintuplicate.

## 3. Results and discussions

### 3.1. Synthesis and Characterization of LaLDHs

The XRD patterns showed in Figure 1a feature reflections characteristic of Mg-Al LDHs and LaLDHs. The characteristic absorption peaks at 2θ values of 11.2$^o$, 22.4$^o$, 34.2$^o$, 60.1$^o$, and 61.4$^o$ correspond to the reflections of (003), (006), (012), (110) and (113) respectively, indicating that the as-prepared Mg-Al LDHs and LaLDHs share a hydrotalcite structure [25, 26]. However, the diffraction peaks at 15.5$^o$, 27.3$^o$, 28.1$^o$, 29.5$^o$, 39.4$^o$, 48.6$^o$ and 56.4$^o$ of the LaLDHs are attributed to the characteristic peaks of $La(OH)_3$, implying that LaLDHs with different $La^{3+}$ / $Al^{3+}$ molar ratio are successfully synthesized and result in different crystalline structures with Mg-Al LDHs.

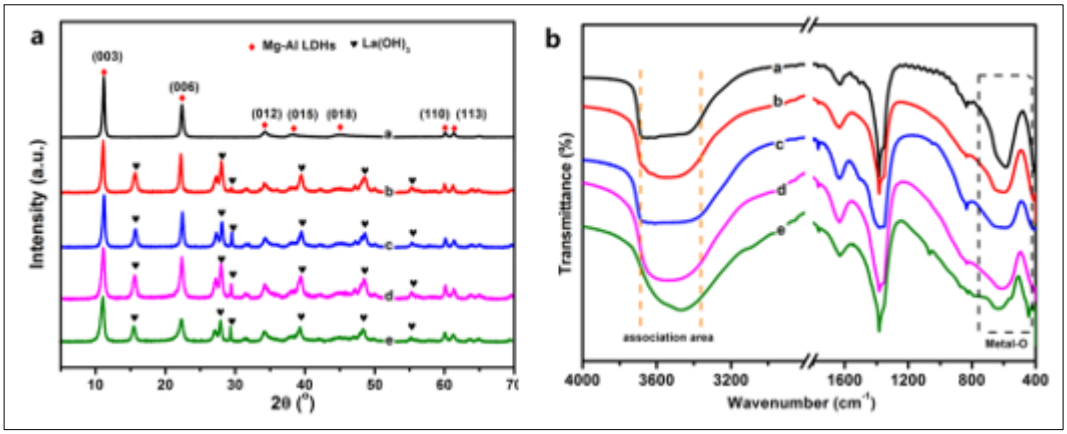


**Figure 1.** XRD patterns (a) and FTIR spertra (a) of Mg-Al LDHs and LaLDHs with different $La^{3+}$ / $Al^{3+}$ molar ratios. (a) pure Mg-Al LDHs; (b) LaLDHs1; (c) LaLDHs2; (d) LaLDHs3; (e) LaLDHs4

Figure 1b presents the FTIR spectra of Mg-Al LDHs and LaLDHs. The broad absorption peak around 3350 $cm^{-1}$to 3630 $cm^{-1}$ is attributed to the –OH stretching modes of the hydroxide layer. The reason for this is that the interlaminar $H_2O$ and –OH in hydrotalcite structure react through the association of H-bond. The interlayer $H_2O$ bending vibration is located at ~1630 $cm^{-1}$ because of H-bond interactions and metal ion coordination. The characteristic peak of $CO_3^{2-}$ appears at ~1370 $cm^{-1}$, as compared with $CO_3^{2-}$ of $CaCO_3$ (1470 $cm^{-1}$) suggesting that there is an intercalation between $CO_3^{2-}$ and interlaminar $H_2O$ through H-bond. The absorption peak in the low wavenumber region at 400 ~ 750 $cm^{-1}$ is assigned to LDH lattice vibrations (Metal-O) [26]. The intensity of Metal-O peaks of LaLDHs (curves of b, c, d, e in Figure 1b) is weaker than that of Mg-Al LDHs (Figure 1b a), indicating that the lattice structure of Mg-Al LDHs is partially replaced by $La^{3+}$. Combined with the results of XRD, it can commonly be believed that $La^{3+}$ has been introduced into the lattice of hydrotalcite.

The morphology and the corresponding particle size of LaLDHs with different $La^{3+}$ / $Al^{3+}$ molar ratios are observed by SEM and TEM. As shown in Figure 2, LaLDHs1, LaLDHs2, LaLDHs3 and LaLDHs4 present uniform, plate-like, well-crystallized nanoparticles with a lateral size around 100-180 nm. Meanwhile, the rod-like $La(OH)_3$ appears on the surface of nanoparticles as the $La^{3+}$ / $Al^{3+}$ molar ratio increases. It can be seen that the nano-rods $La(OH)_3$ and nanoparticles LaLDHs2 exhibit better dispersion and sheet size than others when the $La^{3+}$ / $Al^{3+}$ molar ratio is 1 / 3. Ideal dispersion and sheet size will support a good foundation for follow-up performance of the PVC/LaLDHs nanocomposites [27, 28].

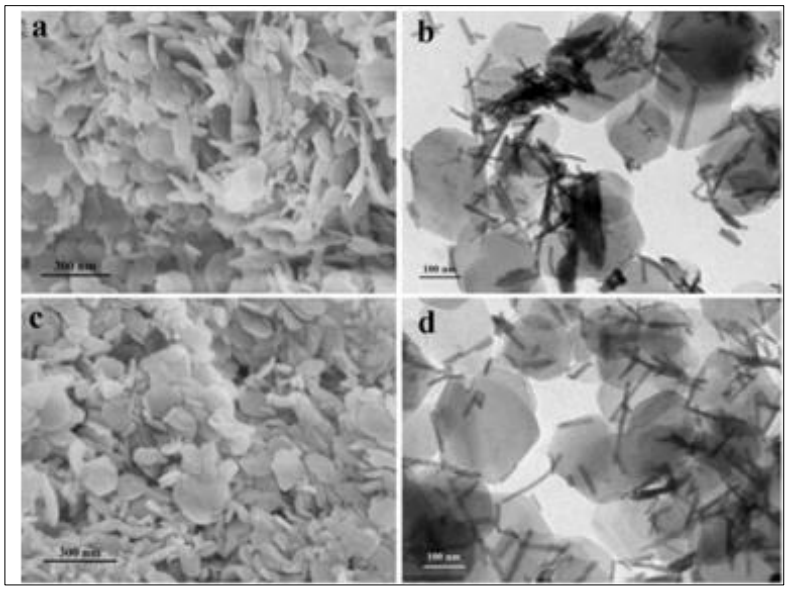


**Figure 2.** SEM and TEM images of LaLDHs. (a, b) LaLDHs1; (c, d) LaLDHs2

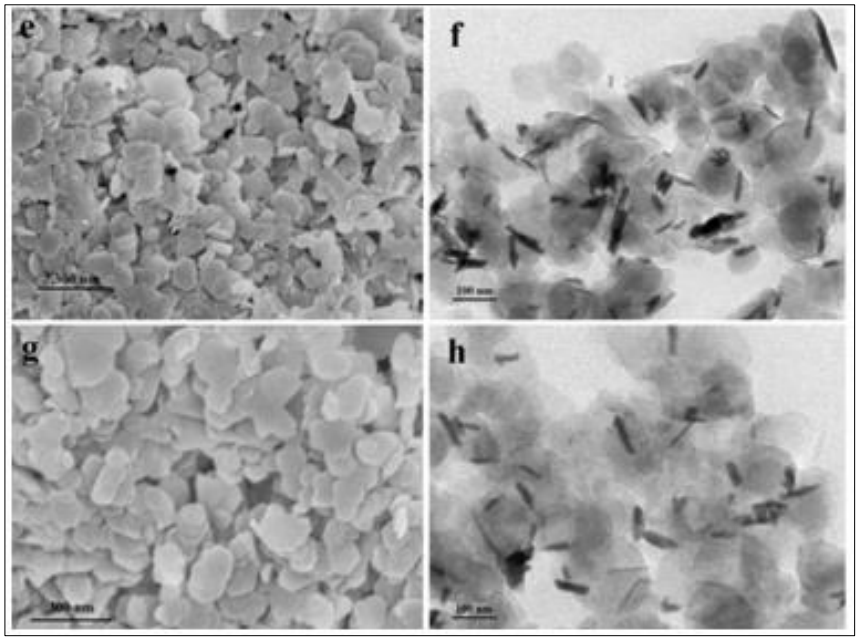


**Figure 2.** SEM and TEM images of LaLDHs. (e, f) LaLDHs3; (g, h) LaLDHs4

### 3.2. Thermal stability performance of PVC-LaLDHs nanocomposites

As we known, different morphologies and sheet sizes of LDHs could significantly affect the thermal stability, smoke-suppression, and mechanical properties of PVC nanocomposites [29, 30]. Based on this contribution, the thermal degradation behavior of PVC-LaLDHs nanocomposites was investigated using TGA, as shown in Figure 3 and Table 1. It can be seen that the shape of the TGA curves for the PVC nanocomposites are different to that of the pure PVC. Obviously, the initial decomposition temperature of PVC-LaLDHs nanocomposites is lower than that of the pure PVC due to the weight loss of LDHs at low temperature [14, 31]. However, all of PVC-LaLDHs nanocomposites and PVC Subsequently suffer two major loss stages. The stage in the temperature range of 240 - 375$^{o}$C is assigned to the dehydrochlorination of PVC and volatilisation of the plasticiser. The next stage at above 415$^{o}$C is from pyrolysis reactions that ultimately lead to char residue. From the Figure 3 and Table 1, it can be found that all the $T_{50\%}$ of nanocomposites increased obviously after loading of LaLDHs. The $T_{50\%}$ values increase from 317.1 $^{o}$C for pure PVC to 324.7$^{o}$C, 334.3$^{o}$C, 337.2$^{o}$C, 330.5 and 330.3$^{o}$C for PVC-LDHs, PVC-LaLDHs1, PVC-LaLDHs2, PVC-LaLDHs3 and PVC-LaLDHs4, respectively. However, compared to pure PVC, the $T_{10\%}$ of the PVC nanocomposites decreased. This is principally because of lower the decomposition temperature of LaLDHs promoting catalysis effect of LaLDHs as a weak alkaline for the degradation of PVC to a small extent. As seen in the Figure 3b, all of LaLDHs composites exhibit much better than LDHs composite in terms of their thermal stability for PVC. The $T_{50\%}$ value increases by 20.1$^{o}$C for PVC-LaLDHs2 compared to pure PVC while it only increases by 7.6$^{o}$C for PVC-LDHs. Additionally, it is worth noting that the $T_{50\%}$ value of the PVC-LaLDHs nanocomposites varies with the change of $La^{3+}$ / $Al^{3+}$ molar ratio, and displayed the highest $T_{50\%}$ value (337.2 $^{o}$C) when the $La^{3+}$ / $Al^{3+}$ molar ratio was indicating that LaLDHs2 tend to improve the thermal stability of PVC more effective.

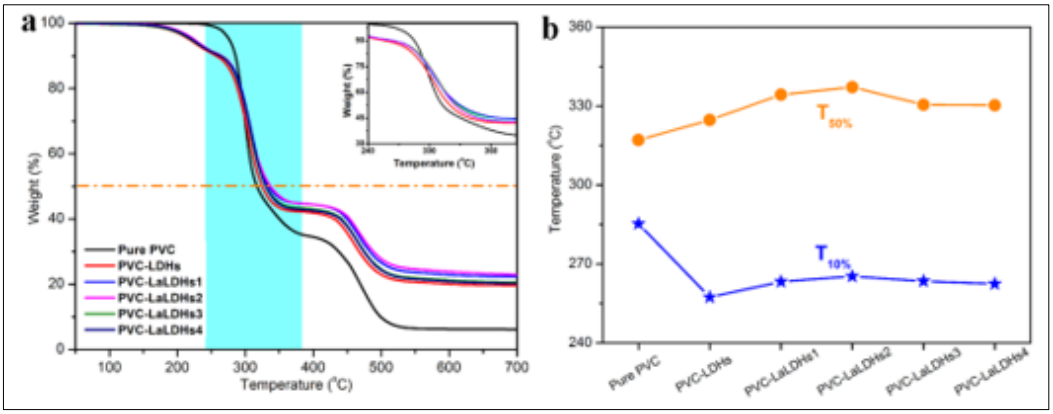


**Figure 3.** TGA analysis of (a) PVC and its composites; (b) a graph of $T_{10\%}$, $T_{50\%}$ vs. PVC and its composites

**Table 1.** TGA analysis results of PVC and its composites

| Sample | [a]$T_{10\%}$ / °C | [b]$T_{50\%}$ / °C | [c]$\Delta T_{50\%}$ / °C |
|---|---|---|---|
| Pure PVC | 285.3 | 317.1 | NA |
| PVC-LDH | 257.4 | 324.7 | 7.6 |
| PVC-LaLDHs1 | 263.3 | 334.3 | 17.2 |
| PVC-LaLDHs2 | 265.3 | 337.2 | 20.1 |
| PVC-LaLDHs3 | 263.5 | 330.5 | 13.4 |
| PVC-LaLDHs4 | 262.5 | 330.3 | 13.2 |

[a]$T_{10\%}$ = temperature at 10% weight loss; [b]$T_{50\%}$ = temperature at 50% weight loss; [c]$\Delta T$ = difference between pure PVC and its nanocomposites.

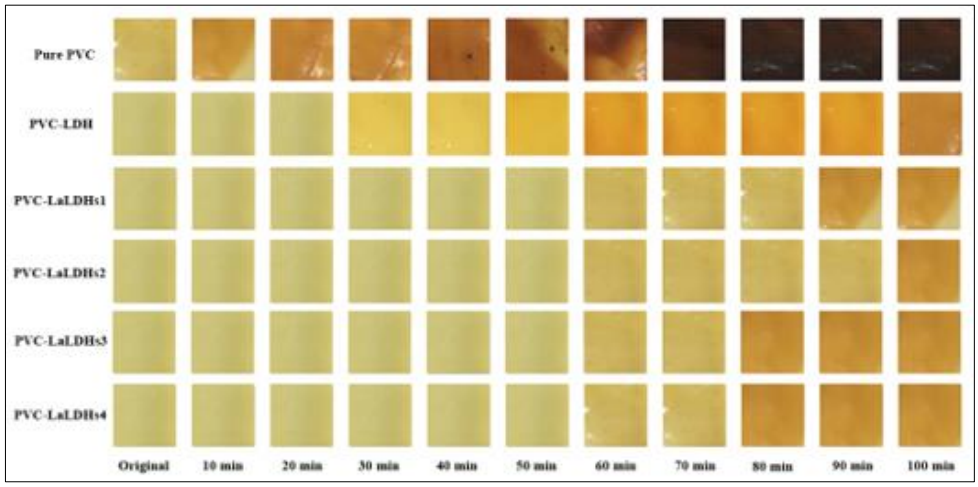


**Figure 4.** Digital photos of PVC and its composites after static thermal aging test at different time

The effect of LDHs and LaLDHs as heat stabilizer on the thermal stability of PVC is illustrated in Figure 4 by static thermal aging test and the Congo red test data of PVC, PVC-LDH and PVC-LaLDHs nanocomposites (Figure 5), respectively. From Figure 4, it can be seen that pure PVC without any stabilizer begins to color even during melt process and becomes completely black after 70 min. The result of Congo red test is also provided that the thermal stability time (TST) of pure PVC is only 1242 seconds (as shown in Figure 5). It is well known that the PVC, under the influence of temperature and radiation, suffers from the autocatalytic dehydrochlorination reaction and HCl catalytic reaction [10].

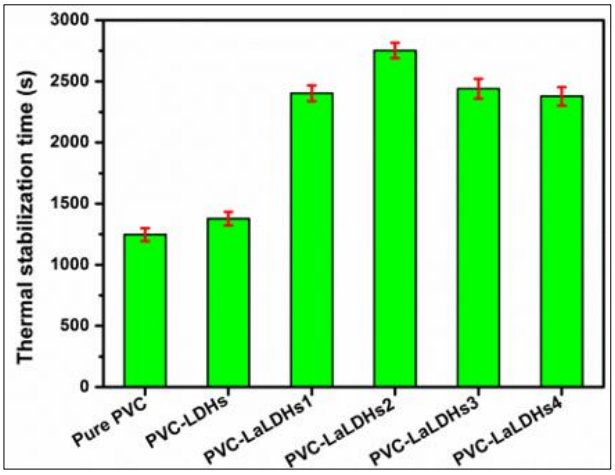


**Figure 5.** Thermal stability of PVC and its nanocomposites as determined by Congo red test (at 195°C±1)

As as-prepared LDHs serves as heat stabilizer for PVC-LDHs, the thermal stability of PVC-LDHs is significantly enhanced with resisting initial coloring. The color turns light yellow appearing at 30 min, and then brown all after 60 min. The main reason is attributed to the addition of as-prepared LDHs that can react with HCl during thermal dehydrochlorination of PVC, and further inhibit the autocatalytic degradation of PVC [11]. However, the TST of Congo red test is increased slightly (1378 s, shown in Figure 5), indicating that the $Cl^-$ produced during thermal degradation of PVC have no enough time to replace the $CO_3^{2-}$ in the interlayer of LDHs.

The thermal stability results of PVC-LaLDHs with different $La^{3+}$ / $Al^{3+}$ molar ratios are also described in Figure 4 and Figure 5, respectively. Compared to PVC-LDHs, the effect of LaLDHs for PVC on the long-term thermal stability is more outstanding. Furthermore, the thermal stability of PVC-LaLDHs composites has a great relationship with the variational $La^{3+}$ / $Al^{3+}$ molar ratio. When the $La^{3+}$ / $Al^{3+}$ molar ratio is 1 / 2, the color of PVC-LaLDHs1 composites turns light yellow extending to 80 min, revealing that the thermal stability of PVC-LaLDHs1 is improved significantly. As the $La^{3+}$ / $Al^{3+}$ molar ratio comes to 1 / 3, the discoloration time of PVC-LaLDHs2 is prolonged to 90 min, illustrating that the PVC-LaLDHs2 possess better thermal stability than that of PVC-LaLDHs1. However, further increment of $La^{3+}$ / $Al^{3+}$ molar ratio (higher than 1 / 3) cannot enhance the thermal stability while weaken it instead (such as PVC-LaLDHs3 and PVC-LaLDHs4), indicating that the optimum $La^{3+}$ / $Al^{3+}$ molar ratio is 1 / 3. The results also are in accordance with that in Congo red test. Therefore, it suggests that the optimum molar ratio of $La^{3+}$ / $Al^{3+}$ is 1 / 3.

As seen in Figure 5, therefore, the PVC-LaLDHs2 exhibits highest TST values of 2752s, and is over 2-times higher than that of pure PVC and nearly 2-fold higher than that of PVC-LDHs, respectively. It is attributed to the strong complexing property and synergistic effect of La element which have long atom radius and more coordination numbers [9]. Relevantly, the La ions ($La^{3+, 4+}$) can react with the labile $Cl^-$ to form a stable coordinate complex, that inhibiting further dehydrochlorination of PVC [10, 22, 32]. Meanwhile, La ions with special electron orbital endow more coordination number, which makes La ions have stronger and more stable bonding with Cl ions. According to the unique synergistic effect of La ions on thermal stability of composites, it is indicated that the optimum molar ratio of $La^{3+}$ / $Al^{3+}$ is 1 / 3 and the as-prepared sample LaLDHs2 with this molar ratio of $La^{3+}$ / $Al^{3+}$ has the best morphology and the corresponding structure as demonstrated in Figure 2.

### 3.3. Smoke density test of PVC-LaLDHs nanocomposites

Necessarily, the smoke density (SDR) is one of the important issues of evaluating the fire hazard of materials. The SDR data and curves of PVC as well as its nanocomposites are shown in Figure 6. From Figure 6a, the SDR of all PVC nanocomposites is lower than that of pure PVC, and fluctuates significantly with types of LDHs and LaLDHs. When the combustion time is less than 50s, the SDR of PVC nanocomposites decreases with the decreased molar ratio of $La^{3+}$ / $Al^{3+}$, indicating that sufficient

amount of La ions has excellent smoke suppression and synergistic effect. However, the SDR of PVC-LaLDHs1 further increases after burning 50s, which may be caused by the morphology and the corresponding structure of LaLDHs1. In Figure 6b, the SDR of PVC nanocomposites decreases firstly and then increases with an increase of $La^{3+}$ / $Al^{3+}$ molar ratio. The maximum SDR of PVC-LDHs, PVC-LaLDHs1, PVC-LaLDHs2, PVC-LaLDHs3, and PVC-LaLDHs4 are 69.1%, 54.7%, 45.6%, 57.7%, and 61.4%, respectively. It is worth noticing that the ΔSDR value of PVC nanocomposites between PVC-LaLDHs2 and pure PVC reaches at 33.1%. The result is probably brought about by the unique synergistic effect, which catalyze forming the high-crosslinking PVC pyrolysis products. Thus, it can promote the formation of char residue and suppress the SDR of PVC-LaLDHs2. It also clearly implies that LaLDHs behaves a great smoke suppression effect as La catalyzed the char layer when the molar ratio of $La^{3+}$ / $Al^{3+}$ is 1 / 3.

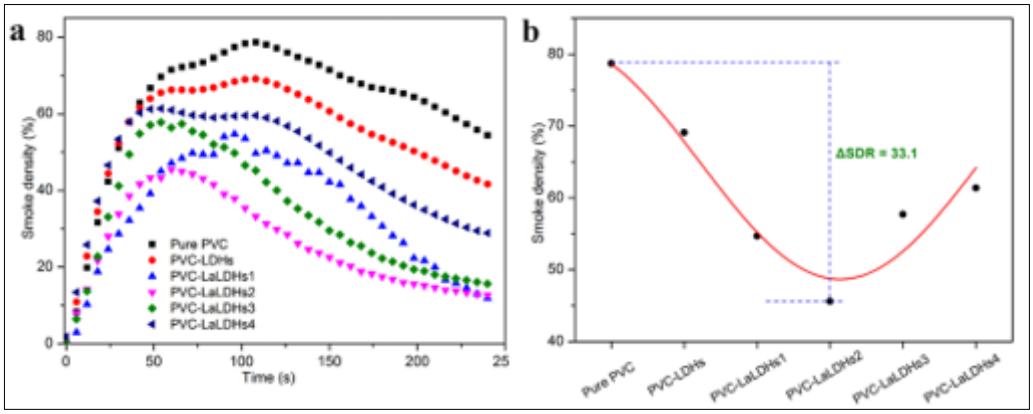


**Figure 6.** (a) Smoke density data of PVC and its nanocomposites;
(b) a graph of maximum SDR vs. PVC and its nanocomposites

### 3.4. Mechanical properties of PVC-LaLDHs nanocomposites

The mechanical properties of PVC and its nanocomposites are presented in Figure 7 and Table 2. In the case of pure PVC, it displays typical ductile fracture with the highest elongation at break ($\varepsilon$, 47.6%) and the smallest tensile strength ($\sigma$, 30.7 MPa) as well as the lowest elastic modulus ($E$, 580.7 MPa) among the nanocomposites. On the contrary, introduction of LDHs to PVC results in a decrease in elongation to 30.7%, while the $\sigma$ gets the highest value of 57.4 MPa, which is caused by the rigidity of LDHs as well as the poor compatibility of LDHs with PVC. As for PVC-LaLDHs, addition of LaLDHs to the PVC matrix effectively improves the $\sigma$ and $E$ of the nanocomposites compared to that of pure PVC, meanwhile, do not have an obvious impact on the decrease of $\varepsilon$. Consequently, the most favorable performance may be observed in case of application of LaLDHs in the PVC. PVC-LaLDHs1 shows a similar $\sigma$ and $E$ to PVC-LDHs. However, the $\varepsilon$ of PVC-LaLDHs1 is much higher than that of PVC-LDHs, possibly due to the effect of LaLDHs1 on the crystallinity of PVC combining with the catalysis of La atom. Noticeably, with increasing $La^{3+}$ / $Al^{3+}$ molar ratio to 1 / 3, the $\varepsilon$ of PVC-LaLDHs2 increases to 40.7 %, which is ~ 1.3-fold higher than that of PVC-LDHs. Meanwhile, the $\sigma$ (56.6 MPa) and $E$ (1017.4 MPa) almost keep the same as PVC-LDHs. Subsequently, the mechanical properties of PVC nanocomposites decrease gradually with further increasing $La^{3+}$ / $Al^{3+}$ molar ratio, which results forming increased agglomeration of LaLDHs and decreased compatibility between PVC and LaLDHs. Consequently, PVC-LaLDHs2 shows the optimum comprehensive mechanical properties, and considered to be the optimum nanocomposite with optimal thermal stability and smoke-suppression effect.

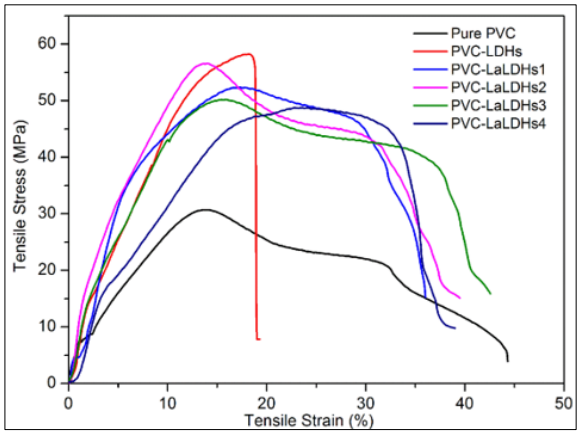


**Figure 7.** Typical stree-strain curves of PVC and PVC-LaLDHs composites

**Table 2.** Mechanical properties of PVC and its composites

| Run | [a] $\sigma_t$ (MPa) | [a] $E$ (MPa) | [a] $\varepsilon$(%) |
|---|---|---|---|
| Pure PVC | 30.7 ± 1.46 | 580.7 ± 21.6 | 47.6 ± 4.3 |
| PVC-LDH | 57.4 ± 4.15 | 935.8 ± 50.3 | 30.7 ± 3.5 |
| PVC-LaLDHs1 | 52.4 ± 3.23 | 825.6 ± 44.7 | 41.6 ± 4.8 |
| PVC-LaLDHs2 | 56.6 ± 1.48 | 1019.4 ± 27.8 | 40.7 ± 3.4 |
| PVC-LaLDHs3 | 50.2 ± 1.84 | 995.3 ± 35.2 | 42.5 ± 3.2 |
| PVC-LaLDHs4 | 49.3 ± 3.22 | 733.5 ± 67.7 | 39.1 ± 5.2 |

[a] $\sigma_t$, $E$, and $\varepsilon$ refer to tensile strength, elastic modulus, and elongation at break, respectively.

[a] $\sigma_t$, $E$, and $\varepsilon$ refer to tensile strength, elastic modulus, and elongation at break, respectively.

### 3.5. Morphological studies of PVC-LaLDHs nanocomposites

As we know the structure of composites determines their properties, especially such as homogeneity of dispersion of filler particles in the polymer matrix, and bonding strength on the interface between the filler particles and matrix. Figure 8 shows the SEM images for the tensile fractured surfaces of pure PVC, PVC-LDHs, PVC-LaLDHs2, and PVC-LaLDHs4. Pure PVC exhibits frizzy and rough surface with evident plastic deformation. For the PVC-LDHs nanocomposite, it shows different behaviors and deformation steps during tensile process (Figure 8a). Because the LDHs particles can be seen as stress concentrated sites for the high stiffness, the followed concentrated stress can promote LDHs particles to undergo the tensile stress. However, the interfacial debonding of the LDHs particles from the PVC matrix easily displays with many voids due to the poor compatibility and interfacial adhesion. In addition, LDHs particles abundantly agglomerate in the PVC matrix (orange circle and arrow in Figure 8b), indicating poor dispersion of LDHs. As a result, the tensile strength and elastic modulus are increased while elongation at break is lost. As the PVC-LaLDHs2, less voids and some twist as well as almost homogeneous surface are found (Figure 8c), suggesting that the LaLDHs2 particles have better dispersion and interfacial adhesion with PVC than others. Thus, the PVC-LaLDHs2 exhibits satisfying strength and toughness. It is supposed that appropriate amount of La ions in composites can catalyze and generate complex with PVC [22, 29, 32], which increase tensile strength and elastic modulus with little affecting elongation at break of PVC. As $La^{3+}$ / $Al^{3+}$ molar ratio increases to 1 / 5, PVC-LaLDHs4 still shows obvious ductile fractured characteristics but agglomeration within the PVC matrix, implying that the dispersion between LaLDHs4 particles and PVC is poorer than that of LaLDHs2 in PVC. However, thanks to the effect of La ions, the PVC-LaLDHs4 composites maintain a comforting elongation at break. Consequently, the homogeneous dispersion between LaLDHs particles and PVC together with optimum $La^{3+}$ / $Al^{3+}$ molar ratio ensure to obtain PVC nanocomposites with optimal comprehensive properties.

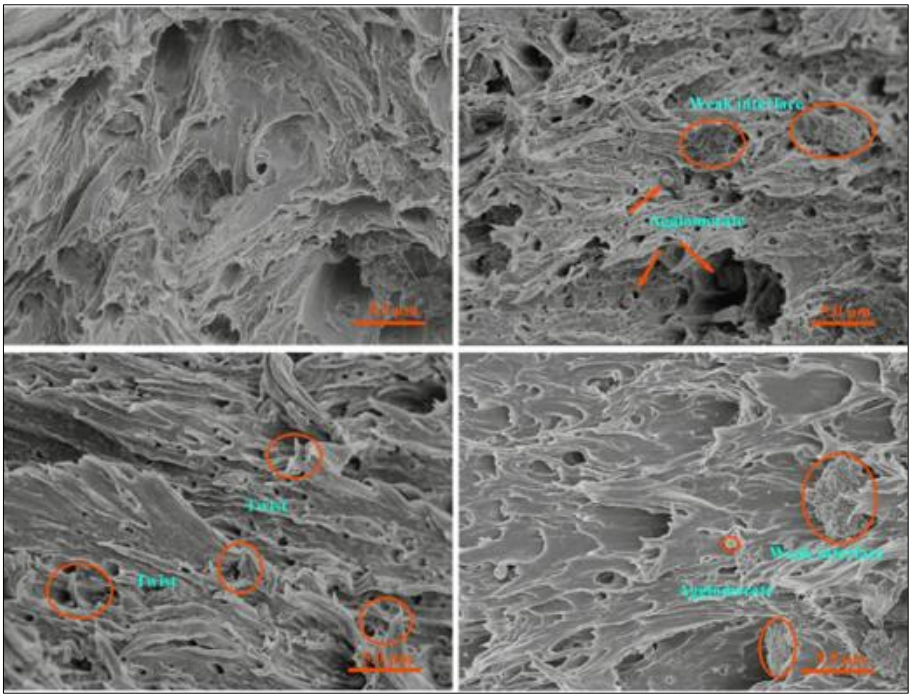

**Figure 8.** SEM images of fracture morphology of (a) pure PVC; (b) PVC-LDHs;(c) PVC-LaLDHs2; (d) PVC-LaLDHs

## 4. Conclusions

In this study, we have successfully synthesized novel La doping Mg-Al layered double hydroxides (LaLDHs) with varying molar ratio of $La^{3+}$ / $Al^{3+}$ via coprecipitation-hydrothermal method. The as-prepared plate-like LaLDHs have well- crystallized structure with a lateral size around 100-180 nm, and exhibit different morphologies for different molar ratio of $La^{3+}$ / $Al^{3+}$. It was further verified that as-prepared LaLDHs can be used for improving thermal stability, smoke suppression and mechanical properties of PVC composites. Especially, introduction of the LaLDHs2 with $La^{3+}$ / $Al^{3+}$ molar ratio of 1 / 3 to PVC has optimum comprehensive properties (including thermal stability, smoke suppression and mechanical properties) compared to other PVC nanocomposites. Adding 2 wt% LaLDHs2 can significantly increase the $T_{50\%}$ of nanocomposites by 20.1$^{o}$C and prolong the thermal aging time (90 min) and TST (2752s), as well as reduce the SDR value of PVC by 33.1%, while the pure PVC leads extremely poor thermal stability (the $T_{50\%}$, thermal aging time and TST are 317.1$^{o}$C, less than 10 min and 1242s respectively) and great SDR value of 78.7%. Moreover, as compared with the pure PVC, PVC-LaLDHs respectively increase the tensile strength and elastic modulus by 84.4% (56.6 MPa) and 75.5% (1019.4 MPa) with little affecting elongation at break of PVC, due to the homogeneous dispersion between LaLDHs particles and PVC together with optimum $La^{3+}$ / $Al^{3+}$ molar ratio. Thus, the as-prepared LaLDHs, especially LaLDHs2, is a new-generation high-efficiency heat stabilizer combining excellent smoke suppression and mechanical reinforcement. More importantly, it would be advantageous to conduct further research on the optimization of rare-earth doped LDHs.

**Acknowledgments:** The authors would like to acknowledge the financial support from Scientific Research Foundation of Zhejiang A&F University (No. 2017FR017), National Natural Science Foundation of China (No. 51903222) and Student Scientific Research Training Project of Zhejiang A&F University (No. 201910341017, No. 202360000402).

**References**

1.ZHANG, B., JIANG, Y., HAN, J., The core-double-shell microcapsules flame retardant: Synthesis and its application for polyvinyl chloride composites, *J. PhyS. Chem. Solids.*, **111**, 2017, 391-402.

2.ZHANG, X., ZHAO, T., PI H., GUO, S., Preparation of intercalated Mg-Al layered double hydroxides and its application in PVC thermal stability, *J. Appl. Polym. Sci.*, **124**, 2012, 5180-5186.
3.KAR, M., YERN CHEE, C., GAN, S.N., Effect of Palm Oil Bio-Based Plasticizer on the Morphological, Thermal and Mechanical Properties of Poly(Vinyl Chloride), *Polymers*, **7**, 2015, 2031-2043.
4. LIU, C., LUO, Y., JIA, Z., LI, S., HUANG, D., JIA, D., Particle configuration and properties of poly (vinyl chloride)/halloysite nanotubes nanocomposites via in situ suspension polymerization, *Polym. Compos.*, **35**(5), 2014, 856-863.
5.KLAPISZEWS, Ł., TOMAZEWSKA, J., SKORCZEWSKA, K., JESIONOWSKI T., Preparation and characterization of eco-friendly Mg $(OH)_2$ / lignin hybrid material and its use as a functional filler for poly (vinyl chloride), *Polymers*, **9**(7), 2017, 258.
6.HIRSCHLER, M.M., Poly(vinyl chloride) and its fire properties, *Fire. Mater*., **41**, 2017, 993-1006.
7.LABUSCHANGE, F.J., MOLEFE, D.M., FOCKE, W.W., DER WESTHUIZEN, I.V., WRIGHT, H.C., ROYEPPEN, M.D., Heat stabilising flexible PVC with layered double hydroxide derivatives, *Polym. Degrad. Stab*., **113**, 2015, 46-54.
8.WAKABAYASHI, K., Register R.A., Ethylene/(meth) acrylic acid ionomers plasticized and reinforced by metal soaps, *Polymer*, **47**, 2006, 2874-2883.
9.ZHENG, Y., CAI, W., FU M., WANG, C., ZHANG, X., Rare Earth Stearates as Thermal Stabilizers for Rigid Poly(vinyl chloride), *J. Rare. Earths*, **23**, 2005, 172-177.
10.WEN, R., YANG, Z., CHEN, H., HU, Y., DUAN, J., Zn-Al-La hydrotalcite-like compounds as heating stabilizer in PVC resin, *J. Rare. Earths*, **30**, 2012, 895-902.
11.XU, Z.P., LU, G.Q., Hydrothermal synthesis of layered double hydroxides (LDHs) from mixed MgO and $Al_2O_3$: LDH formation mechanism, *Chem. Mater.*, **17**, 2005, 1055-1062.
12.LI, S., BAI, Z., ZHAO, D., Characterization and friction performance of Zn/Mg/Al-$CO_3$ layered double hydroxides, *Appl. Sur. Sci.*, **284**, 2013, 7-12.
13.SONG, F., HU, X., Exfoliation of layered double hydroxides for enhanced oxygen evolution catalysis, *Nat. commun.*, **5**, 2014, 4477.
14.FAN, G., LI, F., EVANS, D.G., DUAN, X., Catalytic applications of layered double hydroxides: recent advances and perspectives, *Chem. Soc. Rev*., **43**, 2014, 7040-7066.
15. WANG, Z., LI, X., Synthesis of CoAl-layered double hydroxide/graphene oxide nanohybrid and its reinforcing effect in phenolic foams, *High. Perform. Polym.*, **30**(6), 2018, 688-698.
16.LIU, J., CHEN, G., YANG, J., Preparation and characterization of poly (vinyl chloride)/layered double hydroxide nanocomposites with enhanced thermal stability, *Polymer*, **49**, 2008, 3923-3927.
17.WEN, X., YANG, Z., Yan J, XIE, X., Green preparation and characterization of a novel heat stabilizer for poly(vinyl chloride)–hydrocalumites, *RSC. Adv*., **5**, 2015, 32020-32026.
18.TONG, M., CHEN, H., YANG, Z., WEN, R., The effect of Zn-Al-Hydrotalcites composited with calcium stearate and β-diketone on the thermal stability of PVC, *Int. J. Mol. Sci*., **12**, 2011, 1756-1766.
19.WANG, G., YANG, M, Li Z, LIN, K., JIN, Q., XING, C., HU, Z., WANG, D., Synthesis and characterization of Zn-doped MgAl-layered double hydroxide nanoparticles as PVC heat stabilizer, *J. Nanopart. Res*., **15**, 2013, 1882.
20.FOLARIN, O., SADIKU, E., Thermal stabilizers for poly (vinyl chloride): A review, *Int. J. Phy. Sci*., **6**, 2011, 4323-4330.
21.YI, S., YANG, Z.H., WANG, S.W., LIU, D.R., WANG, S.Q., LIU, Q.Y., CHI, W.W., Effects of MgAlCe-$CO_3$ layered double hydroxides on the thermal stability of PVC resin, *J. App. Polym. Sci.*, **119**, 2011, 2620-2626.
22.WEI, N.N., ZENG, P.H., JI, S.F., ZHAO, P.F., LIU, H., LI, C.Y., Effect of Lanthanum Promoter on Structure and Hydrodesulfurization Performance of La-Ni2P/SBA-15 Catalyst, *J. Chin. Soc. Rare Earth*., **29**, 2011, 310-315.
23.FEDOROV, A., CHEKRYSHKIN, Y., GORBUNOV, A., Studies of recycling of poly (vinyl chloride) in molten Na, Ca‖$NO_3$, OH systems, *ISRN. Chem. Eng*., **10**, 2012, 5402-5408.

24.MATUSINOVIC, Z., WILKIE, C.A., Fire retardancy and morphology of layered double hydroxide nanocomposites: a review, *J. Mater. Chem.*, **22**, 2012, 18701-18704.
25. XU, Z.P., LU, G.Q., Hydrothermal Synthesis of Layered Double Hydroxides (LDHs) from Mixed MgO and $Al_2O_3$: LDH Formation Mechanism, *Chem. Mate.*, **17(5)**, 2005, 1055-1062.
26. XU, W.Z., WANG, S.Q., LIU, L., HU, Y., Synthesis of heptamolybdate - intercalated MgAl LDHs and its application in polyurethane elastomer, *Polym. Adv. Tech.*, **27(2)**, 2016, 250-257.
27. AWAD, W.H., BEYER, G., BENDERLY, D., IJDO, W.L., SONGTIPYA, P., JIMENEZGASCO, M.D., MANIAS, E., WILKIE, C.A., Material properties of nanoclay PVC composites, *Polymer*, **50**(8), 2009, 1857-1867.
28. GUERMAZI, N., HADDAR, N., ELLEUCH, K., AYEDI, H.F., Effect of filler addition and weathering conditions on the performance of PVC/$CaCO_3$ composites, *Polym. compos.*, **37**(7), 2016, 2171-2183.
29. WANG, H., LI, Y., WEI, Z., SONG, Y., LIU, Q., WU, C., WANG, H., JIANG, H., Morphology, mechanical property, and processing thermal stability of PVC/La-OMMTs nanocomposites prepared via in situ intercalative polymerization, *J. Vinyl. Addit. Technol.*, **26**, 2020, 97-108.
30. SONG, X.L., WANG, Y., AN, C.W., GUO, X.D., LI, F.S., Dependence of particle morphology and size on the mechanical sensitivity and thermal stability of octahydro-1,3,5,7-tetranitro-1,3,5,7-tetrazocine, *J. Hazard. Mater.*, **159(2-3)**, 2008, 222-229.
31. GUO, S.Z., ZHANG, C., PENG, H.D., WANG, W.Z., LIU, T.X., Structural characterization, thermal and mechanical properties of polyurethane/CoAl layered double hydroxide nanocomposites prepared via in situ polymerization, *Comp. Sci. Tech.*, **71(6)**, 2011, 791-796.
32. YU, J., LI M.X., Preparation and synergistic properties of lanthanum sorbate composite thermal stabilizer, *J. Chin. Soc. Rare Earth*., **37(6)**, 2019, 746-751.

Manuscript received: 9.07.2020